Implementation of image analysis on thermal shock and cavitation resistance testing of refractory concrete

S. Martinovic [a], M. Dojcinovic [b], M. Dimitrijevic [b], A. Devecerski [c],
B. Matovic [c], T. Volkov Husovic [b,*]

[a] *Institute for Technology of Nuclear and other Raw Mineral Materials, Franchet d'Esperey 86, Belgrade, Serbia*
[b] *University of Belgrade, Faculty of Technology and Metallurgy, Karnegijeva 4, POB 3503, Belgrade, Serbia*
[c] *Insitute of Nuclear Science "Vinca", Material Science Laboratory, Belgrade, Serbia*

Abstract

This paper presents monitoring of changes during thermal shock and cavitation testing for low cement concrete that was synthesized and sintered at 1600 °C for 3 h. Water quench test was applied as an experimental method for thermal stability testing. Image analysis of the samples showed some level of deterioration at the surface and inside the samples before water quench test. During the testing, the level of samples destruction was increasing. Damages inside the samples and at the surface during the water quench test were correlated to the number of quench experiments. Models based on the damage level of both the surface and inside the bulk were proposed for calculation of the strength degradation. Cavitation damages of the samples were induced by the modified vibratory cavitation set-up. Mass loss and surface erosion were determined during the experiment. The results indicated excellent thermal shock behavior and resistance to cavitation erosion.
© 2010 Elsevier Ltd. All rights reserved.

Keywords: Refractory concrete; Thermal stability; Cavitation resistance; Image analysis

1. Introduction

In recent decades, unshaped monolithic refractory materials, especially refractory concretes also known as refractory castables, have been increasingly used due to their advantages over shaped refractory bricks of the same class. Refractory concrete is widely used for critically high temperature application in complex constructions, thin sections, and difficult-to-reach areas. Initially, refractory concrete contained aggregate and relatively high cement content; therefore, the content of mixing water was high as well, forming strong bond, high open porosity (up to 20%), and low raw density. Later, the research was directed towards development of low and ultralow cement concrete due to increasing industry requirements: better rheology, superior physical and mechanical properties, and very high thermal shock resistance. Accordingly, different fine and ultrafine fillers (calcined and reactive aluminas, and microsilica) were added to conventional concrete in order to fill the open pore space between the coarse aggregates, as well as to reduce the cement content and amount of mixing water. Also, some dispersing agents had to be added to improve the rheological behavior of the concrete. Adding of deffloculants and fillers enables simple installation of concrete with low water content thus providing high density and low open porosity. Reduced content of cement and therefore lime results in reduced formation of low melting phases with low refractoriness. In comparison to former (conventional) concrete, the concrete with low and ultralow content of cement has improved hot strength, higher thermal shock resistance, lower open porosity, and increased corrosion resistance.[1–6]

A wide range of Al_2O_3 ceramics are commercially available with strength and heat resistance depending on Al_2O_3 content, which is usually in range of 85–99. Alumina is a ceramic material suitable for high temperature application, with good chemical resistance. Al_2O_3 offers good corrosion resistance to many substances, including inorganic and organic acids, molten and dissolved salts, weak alkali solutions, anhydrous ammonia, hydrogen sulphide, hydrocarbons, organic and inorganic sulphides, molten Sr, Ba, Na, Be, Fe, Co, P, As, Sb and Bi,

* Corresponding author. Tel.: +381 11 3370 466; fax: +381 11 3370 488.
E-mail address: tatjana@tmf.bg.ac.rs (T. Volkov Husovic).

Table 1
Chemical composition of the refractory concrete (dried on 105 °C for 24 h).

Content	Al_2O_3	CaO	Fe_2O_3	MgO	Na_2O	K_2O	LOI
(%)	98.11	1.22	0.018	0.02	0.35	<0.001	2.43

and free molecular hydrogen. Alumina is a most widely used engineering ceramic material due to advantages such as high degree of hardness (25 GPa or 9 on the Mohs scale), high melting point (2054 °C), and good electrical and thermal insulation properties.[7–9]

The properties of refractory concrete depend on characteristics of raw materials and processing procedure. Drying and sintering play the most important role since they influence the formation of final microstructure, that is, creation of typical phases, discontinuities, porosities, vacancies, and cracks. The presence of defects in the structure of sintered refractory concrete is considered undesirable because of deteriorating properties of the material, such as strength, wear, corrosion, abrasion, and thermal shock resistance. They occur randomly throughout the structure, producing smaller or bigger variations in values of measured properties. During the service, the refractory concrete is exposed to mechanical loads, sudden temperature changes, abrasion, corrosion, wear, effects of slag and melted metal. Therefore, all defects in the sintered structure and at the surface of the material will increase and propagate until reaching the critical level that leads to degradation of the material properties and eventually, to the breaking of the bulk.[10]

Since the thermal shock resistance of refractory materials determines their application, it is very important to know thermal stability and behavior of the material during sudden temperature changes. Due to increasing requirements of the iron–steel and metal industry and also nuclear engineering, modern refractory concrete structures should provide a sufficiently long time of resistance to high thermal stress after repeated heating and cooling. Therefore, acquainting with thermo-mechanical behavior of the refractory concrete is of particular importance for its application and life-time. In this paper, thermal shock behavior of low cement high alumina concrete samples sintered for 3 h at 1600 °C will be discussed. Water quench test was applied as an experimental technique.[11–13]

Cavitation, one of the mechanisms of liquid erosion characterized by the generation and collapse of vapor structure in liquid, occurs frequently in hydraulic machinery like pumps, turbines, and propellers. The pressure waves emitted during the collapse of vapor structures interact with adjacent solid surfaces, leading to material damage.[14–24] Cavitation damage test is usually used for metallic materials. As many composite and ceramic materials are expected to replace some of the metallic components, the goal of this investigation was to subject the samples of refractory concrete to cavitation testing.

In addition, the goal was also to investigate the possibilities for application of image analysis in monitoring of the changes in the refractory sample during thermal stability and cavitation resistance testing. The results obtained by image analysis showed that level of degradation could be correlated to the number of quench test cycles and duration of the cavitation test.

2. Experimental

2.1. Material

Refractory concrete was prepared using as an aggregate the tabular alumina (*T-60, Almatis*) with maximum particle size of 5 mm and matrix composed of fine fractions of tabular alumina, 5 wt.% of calcium aluminate cement (*CA-270, Almatis*), reactive alumina (*CL-370, Almatis*) and dispersing alumina (*ADS-3 and ADW-1, Almatis*). The concrete was mixed with 4.67 wt.% of water (dry basis) dispersed with citric acid. Particle size distribution was adjusted to theoretical curves based on modified Andreassen's packing model, with a distribution coefficient (*q*) of 0.25. The refractory concrete mixture was cast in steel moulds by vibration. The samples used for mechanical strength and water quench testing were cubes of 40 mm side length, while 40 mm × 40 mm × 15 mm prisms were used for cavitation testing. After demoulding, the samples were cured for 24 h at room temperature and subsequently dried at 110 °C for 24 hours. Then, they were sintered at 1600 °C for 3 h and cooled down to the room temperature inside the furnace. Chemical composition of the samples is given in Table 1 and relevant mechanical properties are given in Table 2.

Refractory concrete should be considered as a two-phase composite, comprised of a matrix surrounding a skeleton of coarse aggregate grains. Based on the reference literature[25–28] all fractions of concrete components lesser than 45 μm make a matrix. Coarser particles (≥45 μm) that make up an aggregate are considered as an inert component, since they do not participate in formation of hydratable phases.[29,30] Among the components of matrix, cement is the most important one as it contains certain amount of CaO. After introduction of water, fine and ultrafine particles of alumina and CaO form calcium aluminate hydratable phases inside the matrix and during the heating (drying and sintering), they undergo the transformation. Phase changes in the matrix caused by temperature increase can be predicted by phase diagrams C–A and C–A–H (Bogue's notation is applied: C is CaO, A is Al_2O_3, and H is H_2O).[25–29,31] In this paper, phase transformations were monitored by XRD of the matrix and SEM analysis of the castable and confirmed the pres-

Table 2
Relevant mechanical properties of the samples.

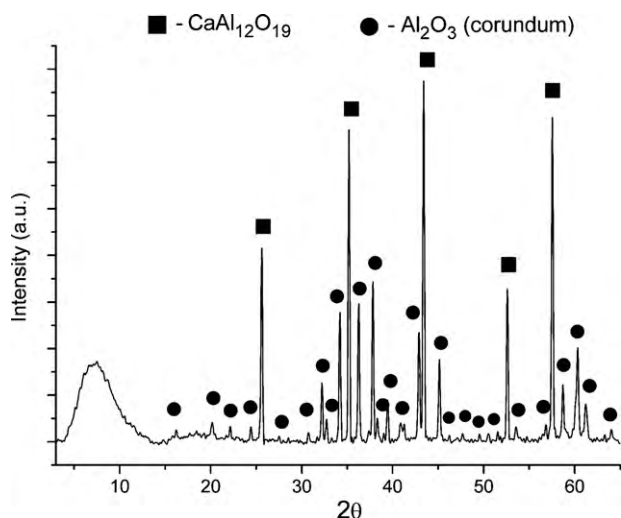| Property	Value
Compressive strength after 20 °C/24 h	59.43 MPa
Compressive strength after drying at 105 °C/24 h	84.37 MPa
Compressive strength after sintering at 1600 °C/3 h	247.17 MPa
Bulk density	3.21 g/cm^3
Water absorption	4.6%
Modulus of elasticity	53.7 GPa

Fig. 1. XRD pattern of the castable matrix sample sintered at 1600 °C/3 h.

ence of the phases described in the literature.[31] XRD analysis of the sample sintered at 1600 °C for 3 h was done, Fig. 1.

XRD pattern confirmed presence of hibonite phase (CA_6), as a high temperature bonding phase as well as newly formed corundum crystals (α-Al_2O_3). Hibonite phase was created by solid phase sintering of fine alumina and calcium aluminate cement during concrete heating and it significantly improved the mechanical strength of the refractory. A and CA_6 phases provided very high ultimate cold crushing and flexural strength, almost four times the value of the reference samples, Table 2. Therefore, assumption that any level of CaO is detrimental in castable systems is not true for all mineral systems. In fact, within the A–C system the formation of CA_6 can be used to yield castables with higher strength.

This paper will present the results of thermal shock stability and cavitation resistance for samples sintered at 1600 °C for 3 h.

2.2. Methods

2.2.1. Water quench test

Thermal shock behavior of the samples was investigated using the water quench test as an experimental method (ICS 81.080 SRPS B.D8.308 former JUS B. D8. 306). The samples were 4 cm × 4 cm × 4 cm cubes. Each thermal shock cycle consisted of several consequent steps: slow heating up at a nominal heating speed of 10 °C/min to the quench temperature set at 950 °C; keeping samples at this temperature for 30 min to reach the thermal equilibrium throughout the specimen volume; and finally, quenching the sample into the water bath at temperature of 23 °C. Experimental method is similar to the procedure described in PRE Refractory Materials Recommendations 1978 (PRE/R5 Part 2). The material exhibited excellent resistance to rapid temperature changes since it withstood 40 cycles without significant degradation of surface and internal structure.

2.2.2. Cavitation test

The cavitation damage level was determined by monitoring of the mass loss and surface degradation during the experiment.

The image analysis of the photographs of sample surfaces using the different software enabled measurement of the surface damage during cavitation erosion.[15–18,21–23] The samples surfaces were marked blue in order to obtain better resolution and to distinguish easier damaged from undamaged surfaces. The results were presented as a surface erosion ratio. The mass loss of the test specimens was determined by analytical balance with an accuracy of ±0.1 mg. Before being weighted, the test specimens were dried in a dryer at 110 °C for 1 h. The measurements were performed after subjecting each test specimen to the cavitation for 30 min. The duration of the tests was 3 h. The erosion parameters were the same as those for metallic samples. The optical microscopy technique was used to analyze the effect of erosion and to interpret the results of cavitation tests.

2.2.3. Image analysis

The image analysis by means of the Image Pro Plus Program was used to determine the destruction level at the surface and inside the bulk of the samples. This is a very convenient method for the determination of damage during thermal shock and cavitation testing. The photographs and microphotographs of samples were taken before and during the tests in order to observe the difference between undamaged and damaged surface of the material during both tests, water quench and cavitation. The samples were marked on the surface by different colors so that better resolution would be obtained and in order to facilitate differentiation between damaged and undamaged surfaces of the material. Five surfaces of the samples were photographed and analyzed in order to measure level of surface deterioration, while the sixth surface was used for marking. The internal structure degradation of the concrete samples during the water quench testing was monitored at the cross sections by using the SEM (scanning electron microscope), type JEOL JSM-5800.

The cross-sections of samples of 5–8 mm in size were prepared by the spattering with nitrogen for 30 min. The changes in surface appearance during water quench and cavitation tests as well as in microstructure inside the samples during the water quench test were detected by image analysis and Image Pro Plus Program. All results were calculated and compared to the ideal surface and finally they were presented in percentages ((P/P_0) 100%). Since certain level of degradation occurred at the surface and inside the bulk even before tests, P_0 was determined according to the ideal facets of 4 cm × 4 cm (16 cm²) in case of surface degradation monitoring and according to the ideal analyzed area of the micrograph in case of detected damage inside the bulk, that is actually the level of porosity adopted as a measure of internal degradation of the bulk.

3. Results and discussion

The changes in appearance of the specimen surface and SEM structures inside the bulk during the water quench testing are presented in Fig. 2. The results of image analysis are given in Fig. 3 as a function of number of water quench cycles. The deterioration level was determined after every 10 cycles.

As it could be seen in Fig. 2, the level of destruction is defined as P/P_0 (P – damaged area and P_0 – undamaged area before

Before testing

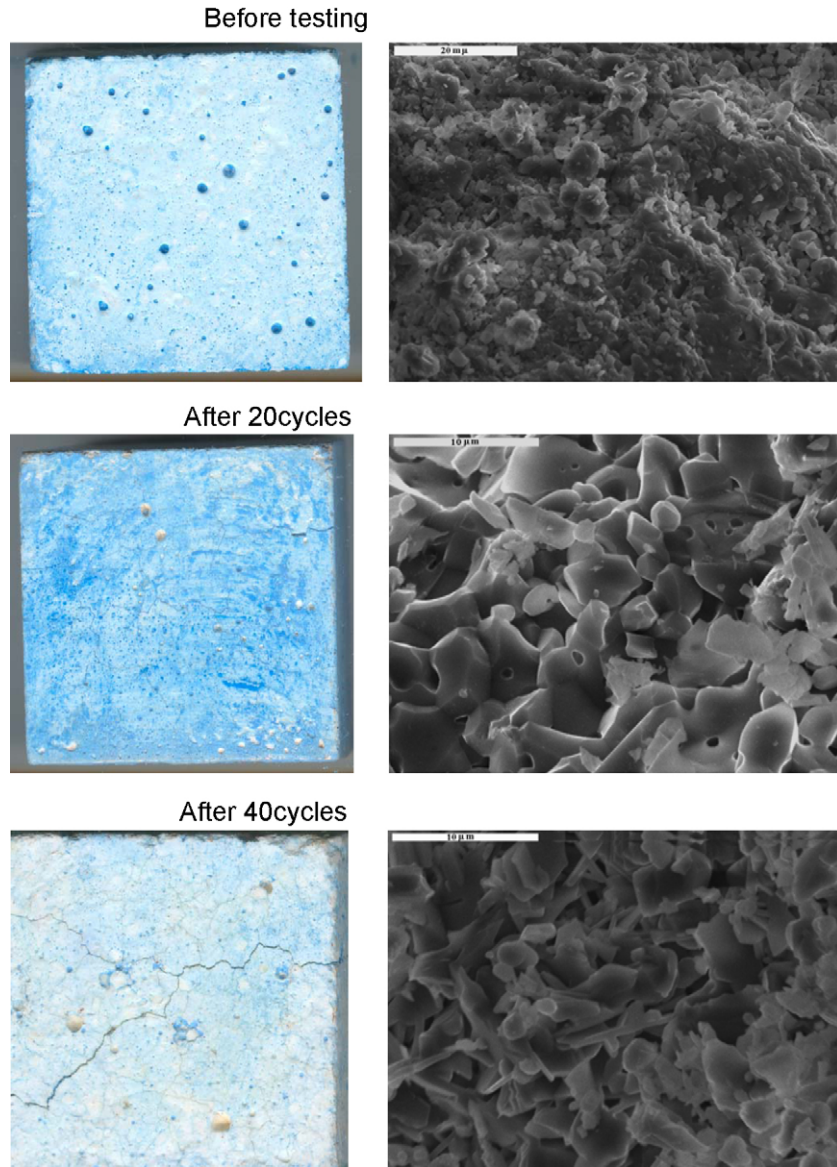After 20cycles

After 40cycles

Fig. 2. Samples before and during water quench test.

quenching), and it is increasing with the number of quench experiments (N). It is important to note that certain level of surface damage was observed before quenching (3.22%) because that affects the thermal shock behavior of the samples, as higher level of destruction will lead to lower thermal stability. The test-
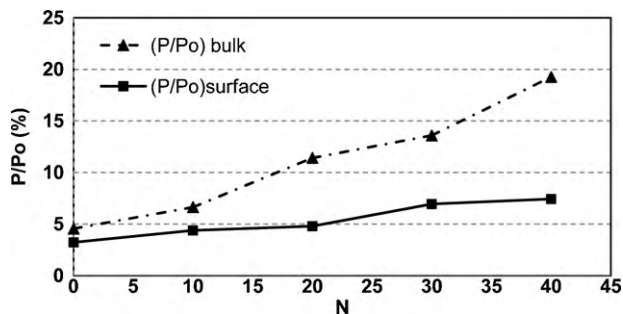

Fig. 3. Damaged surface level (P/P_0) versus number of cycles (N), (P is damaged area and P_0 is undamaged area before testing).

ing consisted of 41 cycles. After 40 cycles of water quenching, the level of surface destruction was below 8%. This low level indicates that the samples exhibited excellent thermal stability behavior. Slightly higher level of damage existed inside the sample before the testing, 4.55%. The tested cubes survived more than 40 cycles with only minor visible fractures at the surface of the samples. It is obvious that surface degradation was not predominant during testing, but degradation inside the bulk. Namely, after 40 cycles, the level of surface degradation was 7.43% while the level of damages inside the bulk was 19.26%. The damage level of both the surface area and inside structure of the sample showed similar trend during the testing, but the damage inside the bulk was occurring faster than at the surface of the sample. It means that spalling effects typical for thermal shock behavior were insignificant in comparison to the influence of inducted stresses inside the bulk that increase with the growing level of damage inside the samples and the number of testing cycles.

The cracks and defects are visible and also detected in the sintered structure before the thermal shock experiments, but it is evident that their propagation during the test happened very slowly. The microstructure of the tested material matrix is characterized by XRD, proving the presence of phases A and CA_6, Fig. 1. CA_6 phase is embedded and distributed inside the Al_2O_3 matrix. Thermodynamically, CA_6 phase is compatible with alumina and it has the same average thermal expansion coefficient ($\approx 8.5 \times 10^{-6} \, ^\circ C^{-1}$). However, the thermal expansion behavior is highly anisotropic, since $\alpha_A = 7.3 \times 10^{-6} \, ^\circ C^{-1}$ and $\alpha_{CA6} = 11.8 \times 10^{-6} \, ^\circ C^{-1}$, so thermal expansion mismatch between A and CA_6 particles may be expected. Difference between thermal expansions of these two phases upon sudden temperature changes can provoke the material anisotropy, generating the thermal stresses that can cause initial formation of micro-cracking around the loaded boundary between two phases and sites for the crack propagation.[32]

The residual stress (P) can be estimated based on Eq. (1)[33,34]:

$$P = \frac{\Delta\alpha\Delta T}{(1 + vm)/2Em + (1 - 2vp)/EP} \tag{1}$$

where $\Delta\alpha$ is the difference between thermal expansion coefficients, ΔT is the quenching temperature range, v is Poisson's ratio, E is the Young modulus and R is the radius of particular phase.

When the thermal expansion coefficient of the secondary phase (CA_6) is higher than of main grains (A), the grain boundary phase (CA_6) is under tensile stresses and the fraction of intergranular fracture is very high. However, it allows a very high toughness due to crack deflections and grain branching around large, elongated grains of A. Because of these mechanisms the material shows good resistance to the thermal shock in spite of cracks presence.

The resistance of the prepared sample to cavitation was determined by measuring of the mass loss as well as surface degradation of the samples. Since refractory concrete with high content of alumina were used, some water absorption was expected. According to the data presented in Table 1, water absorption was 4.6% for the sample sintered for 3 h at 1600 °C. After the first cycle of cavitation experiment (30 min), mass loss was not observed, but the sample mass increased due to
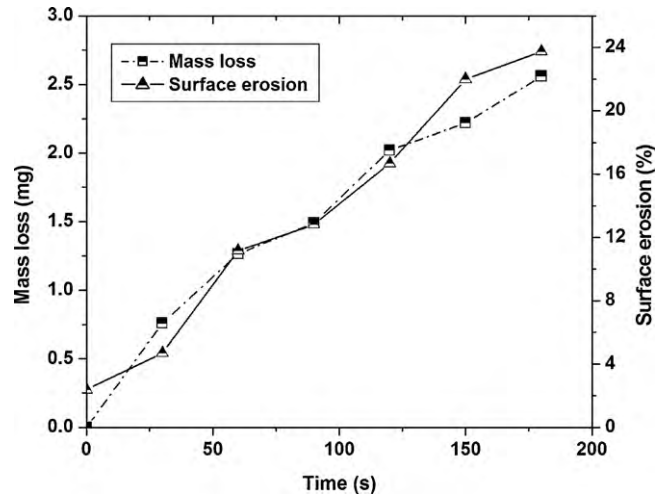

Fig. 4. Mass loss and surface erosion during the cavitation testing.

water absorption. For the quantification of the expected mass loss, after every cycle of experiment the samples were dried at 105 °C until reaching the constant mass. After drying, samples exhibited the expected behavior and the mass loss during the cavitation experiment, which is presented in Fig. 4.

Regarding results presented in Fig. 4, small change in the mass loss was observed. Mass loss during the experiment showed excellent correlation with time. Surface deterioration was observed at the samples; photographs of the samples before and during the experiment are presented in Fig. 5.

Image Pro Plus Program was used for surface analysis and determination of the level of deterioration during the cavitation testing. For better distinction between damaged and undamaged surface areas, the observed sample surface was covered by blue chalk. The damaged area appeared as dark blue and undamaged area as white or lighter shade of blue). The results are given in Fig. 4.

The erosion parameters were the same as those for metallic samples. The obtained results showed that surface erosion was in strong correlation with time: erosion of the sample surface was 0.76% before the testing and below 24% after 180 min of cavitation testing.

The image analysis showed certain level of destruction at the surface and inside the sample before thermal stability test-

Fig. 5. Samples before and during testing: (a) before testing, (b) after 60 min, and (c) after 180 min, Fig. 6. Strength degradation (model with surface damage) versus number of cycles (N)
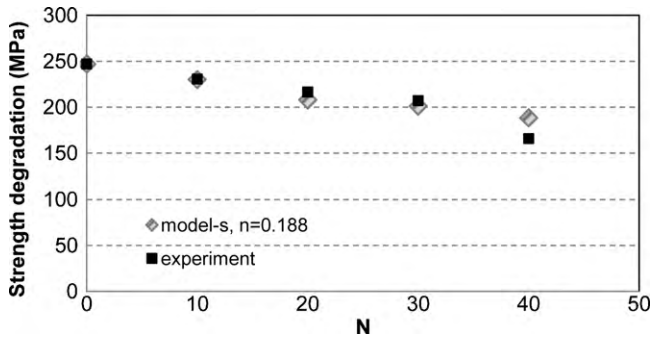
Fig. 6. Strength degradation (model with surface damage) versus number of cycles (*N*).

ing. According to the previous results, model for prediction of strength degradation based on level of degradation is presented:

$$\sigma = \sigma_0 \left(\frac{P}{P_0} \right)^n \qquad (2)$$

where σ is the compressive strength, σ_0 is the strength before quenching, P is the level of destruction, P_0 is the level of destruction before quenching, and n is the coefficient. For Eq. (2) and the results of surface damages and damages inside the samples, coefficient had value $n = 0.188$. The obtained results are presented in Figs. 6 and 7. The results indicated a strong correlation between strength degaradation and number of thermal shock cycles. As expected, the compressive strength was decreasing during the quenching. For presented model validation, experimental values of strength were obtained by using the standard laboratory procedure (cold crushing strength test ICS 81.080 SRPS B. D8. 304). The proposed models showed excellent correlation with experimental values, as well with number of cycles.

The results obtained using the model for prediction of strength degradation based on level of destruction inside the sample showed excellent correlation with experimental results. The proposed model based on measured level of destruction exhibited excellent compliance with the experimental values. As the levels of damage at the surface and inside the sample during the testing were different, the models with the same coefficient n were proposed for determination of surface destruction level or the destruction level inside the sample.
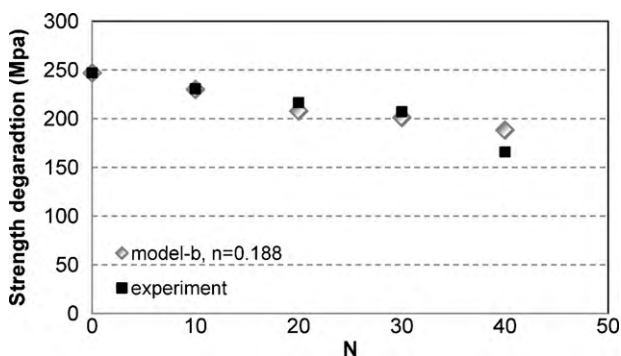

Fig. 7. Strength degradation (model with damage inside the sample) versus number of cycles (*N*).

The cavitation experiment indicated that excellent mechanical characteristics, especially high values of cold crushing strength (Table 2) could lead to good cavitation resistance. The results presented in Figs. 6 and 7 confirmed correlation between mechanical characteristics and cavitation resistance. The image analysis results showed that the level of degradation of samples was increasing during the experiment. After 180 min, the level of surface destruction during cavitation was 23.75%. This level was higher than the level of destruction caused by thermal shock when the damage of the surface was below 10% and below 20% inside the bulk after 40 cycles of thermal shock.

4. Conclusion

The synthesis of the low cement concrete with high content of alumina and its thermal stability and cavitation resistance characterization were the goals of this paper. The tested material was prepared and subjected to sintering temperature of 1600 °C with the dwell time of 3 h. The conclusions are as follows.

Material exhibited excellent thermal stability, as the maximum number of quench experiment was over 40 cycles.

Non-destructive evaluation of surface behavior during the tests was performed in order to monitor the level of destruction by using Image Pro Plus Program.

The results of image analysis of sample surface and inside structure were used for elaboration of the model for strength degradation prediction. In both cases, samples showed an excellent correlation with the number of cycles. Validation of the proposed model was realized by comparing the model results with the experimental data. The proposed coefficient was $n = 0.188$ for both models, one based on surface destruction, and another on destruction inside the sample.

This material exhibited very good cavitation resistance behavior.

The applied non-destructive method (image analysis) showed advantages in monitoring of samples' behavior during thermal stability testing. The results obtained by non-destructive measurements enabled much better monitoring of the sample behavior during the testing. It proved to be very convenient for measurement of the degradation level which is important for better prediction of material behavior, as well as optimum design of materials for specific application where thermal stability and/or cavitation resistance are involved.

The obtained results showed that the investigated material exhibited very good thermal shock and cavitation erosion resistance. The future use of this material can be expected in conditions where cavitation resistance is required.

References

1. Altun IA. Effect of temperature on the mechanical properties of self-flowing low cement refractory concrete. *Cem Concr Res* 2001;**31**:1233–7.

2. Khalil NM, Zawrah MF, Serry MA. Magnesia-spinel-based zero-cement refractory castables. *Ind Ceram* 2005;**25**(2):104–9.

3. Zawrah MFM, Khalil NM. Effect of mullite formation on properties of refractory castables. *Ceram Int* 2001;**27**:689–94.

4. Kakroudi G, Huger M, Gault C, Chotard T. Damage evaluation of two alumina refractory castables. *J Eur Ceram Soc* 2009;**29**:2211–8.

5. Cardoso FA, Innocentini MDM, Miranda MFS, Valenzuela FAO, Pandolfelli VC. Drying behavior of hydratable alumina-bonded refractory castables. *J Eur Ceram Soc* 2004;**24**:797–802.

6. Parr C, Valdelièvre B, Wöhremeyer C. Application of calcium aluminate cement to dense low water demand refractory castables. *Refract Appl News* 2002;**7**(3):17–23.

7. Meетхам GW, Van de Voorde MH. *Materials for high temperature engineering applications*. Springer; 2000.

8. Bengisu M. *Engineering ceramics*. Springer; 2001.

9. Available from: http://www.matweb.com.

10. Leonelli C, Bondioli F, Veronesi P, Romagnoli M, Manfredini T, Pelacani GC, Cannillo V. Enhancing the mechanical properties of porcelain stoneware tiles: a microstructural approach. *J Eur Ceram Soc* 2001;**21**:785–93.

11. Marenovic S, Dimitrijevic M, Volkov Husovic T, Matovic B. Thermal shock damage characterization of refractory composites. *Ceram Int* 2008;**34**(8):1925–9.

12. Marenovic S, Dimitrijevic M, Volkov Husovic T, Matovic B. Thermal shock damage characterization of refractory composites. *Ceram Int* 2009;**35**(3):1077–81.

13. Boccaccini DN, Romagnoli M, Kamseu E, Veronesi P, Leonelli C, Pellacani GC. Determination of thermal shock resistance in refractory materials by ultrasonic pulse velocity measurements. *J Eur Ceram Soc* 2007;**27**(2–3):1859–63.

14. Russell RO, Morrow GD. Sonic velocity quality control of steel plant refractories. *Am Ceram Soc Bull* 1984;**63**(7):911–4.

15. Dojcinovic M, Volkov Husovic T. Cavitation damage of the medium carbon steel: implementation of image analysis. *Mater Lett* 2008;**62**:953–6.

16. Hammit FG. *Cavitation and multiphase flow phenomena*. New York: McGraw-Hill; 1980.

17. Knapp RT, Daily JW, Hammit FG. *Cavitation*. New York: McGraw-Hill; 1970.

18. Okada T, Iwai Y, Hattory S, Tanimura N. Relation between impact load and the damage produced by cavitation bubble collapse. *Wear* 1994;**184**:231.

19. Hattori S, Mori H, Okada T. Quantitative evaluation of cavitation erosion. *J Fluid Eng Trans ASME* 1998;**120**:179.

20. Okada T, Hattori S.*Proceedings of the international symposium on aerospace and fluid science*. 1993. p. 347.

21. Steller K.*Proceedings of the 6th international conference on erosion by liquid and solid impact*. 1983. p. 121.

22. Bregliozzia G, Schinob A, Di, Ahmeda SI-U, Kennyb JM, Haefkea H. Cavitation wear behaviour of austenitic stainless steels with different grain sizes. *Wear* 2005;**258**:503–10.

23. Tomlinson WJ, Bransden AS. Cavitation erosion of laser surface alloyed coatings on Al–12% Si. *Wear* 1995;**185**:59–65.

24. Lin CJ, He JL. Cavitation erosion behaviour of electroless nickel-plating on AlSl 1045 steel. *Wear* 2005;**259**:154–9.

25. Innocentini MDM, Pardo ARF, Pandolfelli VC, Menegazzo BA, Bittencourt LRM, Rettore RP. Permeability of high-alumina refractory castables based on various hydraulic binders. *J Am Ceram Soc* 2002;**85**(6):1517–21.

26. Cardoso FA, Innocentini MDM, Akiyoshi MM, Pandolfelli VC. Effects of curing conditions on the properties of ultra-low cement refractory castables. *Refract Appl News* 2004;**9**(2):12–6.

27. Maitra S, Bose S, Bandyopadhyay N. Dehydration kinetics of calcium aluminate cement hydrate under non-isothermal conditions. *Ceram Int* 2005;**31**:371–4.

28. Studart AR, Pileggi RG, Pandolfelli VC, Gallo J. High alumina multifunctional refractory castables. *Am Ceram Soc Bull* 2001;**80**(11):34–9.

29. Nonnet E, Lequeux N, Boch P. Elastic properties of high alumina cement castables from room temperature to 1600 °C. *J Eur Ceram Soc* 1999;**19**:1575–83.

30. Hommer H, Wutz K, Seyerl JV. The effect of polycarboxylate ethers as deflocculants in castables. *Interceram Refract Man* 2007:46–8.

31. Levin EM, Robbins CR, McMurdie HF. Phase diagrams for ceramists. Compiled at the National Bureau of Standards. *Am Ceram Soc* 1969.

32. Sanchez-Herencia AJ, Moreno R, Baudin C. Fracture behavior of alumina-calcium hexaluminate composites obtained by colloidal processing. *J Eur Ceram Soc* 2000;**20**:2575–83.

33. Liaw HJ, Wei J, Wen–Cheng. Calcium aluminate composites with controlled duplex structures. II. Microstructural development and mechanical properties. *J Ceram Process Res* 2005;**6**(3):230–5.

34. Davidge RW. *Mechanical behavior of ceramics*. London: Cambridge University; 1979.